QUANTIFICATION OF SEASONAL CHARACTERISTICS OF LAND SURFACE TEMPERATURE OVER DELHI USING LANDSAT 8 SATELLITE IMAGERY

Srishti Solanki, J. K. Garg*
University School of Environment Management, Guru Gobind Singh Indraprastha University
Sector- 16C, Dwarka, New Delhi - 110075, India
Email ID: gargjk@gmail.com*

KEY WORDS: Delhi, Urban Heat Island, Land Surface Temperature, Land Use/ Land Cover.

ABSTRACT

The dense-built up areas exhibit higher land surface temperature compared to the surrounding landscape and act as islands of elevated temperatures surrounded by relatively cool suburbs. This phenomenon is defined as Urban Heat Island effect. The present study investigates the current trends of spatial variation in surface temperature over Delhi during summer and winter seasons and assesses the effect of urbanization on the local climate. Delhi is a metropolitan city with reserved forests, protected forests and wildlife sanctuary. However, the concrete areas of Delhi have experienced unparalleled horizontal and vertical growth, leading to major modifications of land use/cover. We used thermal infrared sensor (TIRS) band 10 of Landsat 8 for Land surface temperature retrieval. Different formulas were used to obtain the parameters for land surface temperature (LST) retrieval, i.e., radiance, brightness temperature and emissivity, giving the thermal profile of the ground surface. The mean LST value for Delhi in January and June 2017 was estimated to be 20.68 ˚C and 29.64 ˚C, respectively. In summer, LST ranged from 24.31˚C to 35.32˚C and in winter from 18.31˚C to 23.97˚C, which is much influenced by the existing Land Use/Covers. During summer, the lowest temperature was recorded from surface waterbodies, and the highest temperature was recorded from barren agricultural land and dense urban areas. However, an ideal UHI pattern was observed during winter. Furthermore, the Central Delhi Region and the commercial/industrial areas displayed heat island conditions in summer and winter seasons, with a mean temperature difference of 3.6˚C and 2.9˚C, compared to the suburbs. The surface temperature increment at the city level is mainly due to the joint effect of anthropogenic activities, changes in LULC patterns and vegetation. The results of the study suggest that in the urban area of Delhi, the surface temperature observed is comparatively higher than the surface temperature of rural area.

1. INTRODUCTION:

Urbanization is characterized by the rapid emergence of new cities and increasing population. In 2011, world population increased to 7 billion in 2011, of which 3.6 billion, i.e., more than 50 %, resided in urban areas and the percentage is expected to increase to 60 % by 2030 (Population Reference Bureau, 2004; Dhorde et al., 2009). This has made urbanization a global concern and is receiving widespread attention from planners and policy makers from world over (Singh, 2015). Demands of the population for land and resources are causing outward expansion of cities. This is consuming large areas of agricultural and forest land and pushing the fringe further. This urban sprawl is inevitably accompanied by concretization, industrial growth, traffic congestion, air pollution and much more (Singh, 2015). Deforestation and conversion of the natural land surface into impervious land has resulted in a change of local atmosphere and elevated land surface temperature (Kikon et al., 2016). This land transformation alters the near surface energy budget by reducing evapo-transpiration, crowding solar energy absorbing surfaces, and creating heat-trapping canyon-like urban morphology (Singh, 2015).

The dense-built up exhibits higher land surface temperature (LST) in comparison with the surroundings (Mallick, 2014) resulting in urban warming. As a result, dense-bulit up areas act as islands of elevated temperatures surrounded by the sea of relatively cooler suburbs (Singh et al., 2014). This phenomenon is defined as Urban Heat Island effect, wherein an urban area is comparatively warmer than a surrounding rural area. This event is caused by human-induced modification of land surfaces and additional heat-generating activities associated with urban population (Bhati & Mohan, 2015), leading to urban geometry that stores the shortwave radiation and radiates longwave radiation (Oke, 1982).

UHI is a multi-scaled phenomenon, i.e., it may occur within a city at different size, shape, intensity and time. The amount and distribution of land cover (i.e., vegetation, bare soil, paved area, etc.) and land use (i.e., residential, commercial, industrial) account for variation in temperature across cities and within cities (Alberti, 2008). Other than the morphology and size of the city, the local level meteorological conditions such as relative humidity, cloud cover play a distinctive role in the UHI development, which mainly modulates the diurnal cycle of temperature variations across the city (Roy & Singh, 2015). Surface heat islands are greatest in the day and atmospheric heat

islands in the night (Lo & Quattrochi, 2003). Similarly, many Urban Cool Islands (UCIs) may also exist over vegetated patches in the urban landscape. UHI can be a significant factor for local & regional climatic and environmental changes, leading to a number of social and ecological consequences (Richter & Weiland, 2012). It also contributes to increased heat stress and human mortality (Singh et al., 2014). According to a study conducted by McDonnell et al., 1997, in addition to the increased surface temperature, the urban heat island affects the growth and decomposition rates of plants and microbes. Therefore, there is a need to tackle the growing problem of UHI in Indian cities and to develop efficient UHI mitigation strategies.

In today's world of globalization and industrialization, urban environmental studies have become an important area of research. Satellite Remote Sensing, with its repetitive coverage, is a powerful tool to map and monitor changes in the core and periphery of urban areas (Rahman & Netzband, 2007). Remote sensing satellite data can be utilized to assess urban land surface thermal characteristics through mapping and assessing surface temperature using thermal infrared images (Mallick & Rahman, 2012). Land surface temperature (LST) is a critical parameter in urban climatology and UHI Effect studies. The land use/cover and surface temperature are positively correlated owing to albedo and moisture content of the respective surface type (Singh & Grover, 2015). Estimation of LST from remote sensing data has so many different methods and algorithms, but LST is primarily sensitive to vegetation profile and surface characteristics. Since, emissivity represents surface characteristics, and vegetation can be used to calculate the emissivity, UHIs can be identified on the basis of surface temperature differences.

Delhi, being one of the major metropolitan cities as well as the capital of India, is constantly growing under pressure of urban development. Although, Delhi has the distinction of being one of the few metros that possess reserved forests, protected forests, wildlife sanctuary and city forests (Sinha, 2014), the concrete areas of Delhi have experienced unparalleled horizontal and vertical growth, leading to the major modifications of the land use/ land cover (Singh & Grover, 2015). As per the records of Census of India (2011), Delhi has a maximum density in India, with 11,297 persons/ km^2. Till 1901, Delhi was a small city with a total population of 0.4 million of which 52.76% was urban, which increased to 16.79 million total and 97.50 % urban population by 2011 (Delhi Statistical Abstract, 2014). By 2020, after Mumbai and Tokyo, it is anticipated that Delhi might become the third largest metropolitan region (Anonymous, 2017). Thus, the city needs special focus from planning perspectives but the current trends of growth and development in the city are indicting negative bearings on the environment (Singh, 2015).

The aim of undertaking this study is to investigate the current trends of spatial variation in surface temperature over Delhi during summer and winter seasons, and assess the effect of urbanization on the local climate. For land surface temperature (LST) retrieval an algorithm employing TIRS Band 10 data of Landsat 8 was used. Different formulas were used to obtain the parameters for land surface temperature (LST) retrieval, i.e., radiance, brightness temperature and emissivity, giving the thermal profile of the ground surface. Although the processed Landsat 8 data is available, there is still large calibration uncertainty associated with Band 11, which leads to an error in LST estimation. According to USGS Landsat Website, the calibration variability of Band 10 is 0.12 $w/m^2/sr/\mu m$ (~0.8K) and 0.2 $w/m^2/sr/\mu m$ (~1.75K) for Band 11, which shows that the accuracy for LST Band 10 is higher than LST Band 11 (Yu et al., 2014). In Landsat 8, the stray light, i.e., thermal energy from outside the normal field of view affects the data collected in Bands 10 and 11 of the L8 TIR sensor (Montanaro et al., 2014). Therefore, only Band 10 TIRS data of Landsat 8 has been used in this study for LST estimation.

2. MATERIALS AND METHOD:

2.1. Study Area: Delhi:- City Profile

Delhi, the capital of India (Figure 1 &2), is located in the fertile alluvial plains of Northern India as a riparian city of the River Yamuna, located between 28°24'17" N latitudes and 28°53'00" N latitudes and 76°45'30" E longitude and 77°21'30" E longitude (Sharma & Joshi, 2015). It nestles at cross boundaries of two neighboring states, Haryana and Uttar Pradesh covering an area of approximately 1,483 km^2. The city's altitude ranges from 213 to 305 m (Sharma & Joshi, 2015). For the purpose of governance and management, Delhi city is divided into 11 districts and 33 tehsils/ sub-divisions. Unlike many large growing cities of the Asia, Delhi posses mixed land use/cover comprising of built up area interspersed by layers of tree cover. As per the India State of Forest Report, 2015, Delhi has a forest cover of total 188.77 sq km (12. 73% of total geographical area) (ISFR, 2015). Delhi's forest cover has increased by 8.96 sq km since 2013, which was then recorded as 179.81 sq km (12.12 % of g. a.) (ISFR, 2013). The city is characterized by a semi-arid climate with a stark contrast in the day and night temperatures, high saturation deficit and low to moderate rainfall. There are four major seasons during the year, the summers (March–June), monsoons (June–September), post-monsoons transition (October–November) and winters (November to March). The average temperature is known to vary from 25°C to 45°C during the summer and 22°C to 5°C during the winter (Anonymous, 2014).

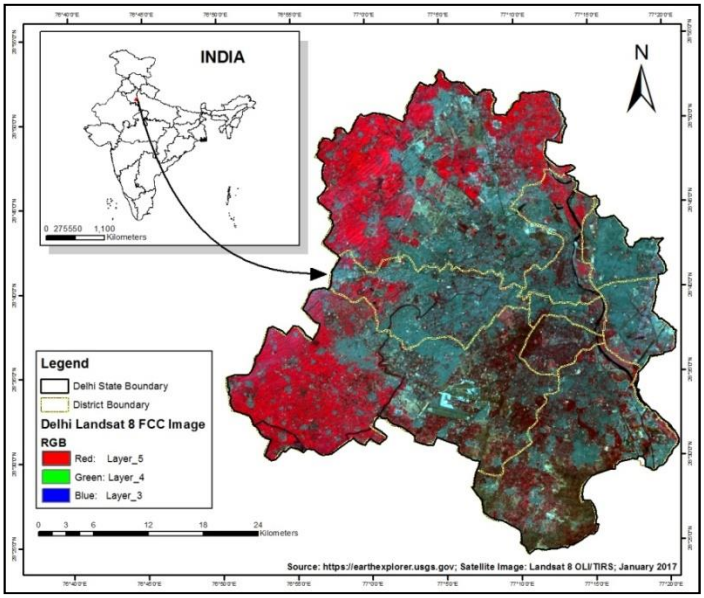

Figure 1: Map showing the location of the study area, Delhi Metropolitan Region.

Geographically, delhi can be divided into three: the Ridge, the Yamuna floodplains, and the plains. Much of the Delhi area is plains. The Delhi Ridge (7784 ha.), an extension of Aravallis into the city, stretches from Delhi University in the north towards Jawaharlal Nehru University in the south and beyond, covering a distance of about 35 km (Srishti, 2014). It is further divided into five parts, i.e., Northern Ridge (87 ha.), Central Ridge (864 ha.), South Central Ridge (626 ha.), Southern Ridge (6200 ha.) and Nanakpura South Central Ridge (7 ha.)(Sinha, 2014).Vegetation of Delhi is characterized by thorny scrub, which is found in arid and semi arid Zone. As per classification of Champion and Seth (1968), the main forest, i.e., Ridge Forest falls in the category of 'Tropical Thorn Forest' and more especially as 'Semi Arid Open Scrub' (Forest Department, GNCTD, 2016). Other than the Ridge, there are 26 protected forests and 42 city forests in Delhi (Sinha, 2014).

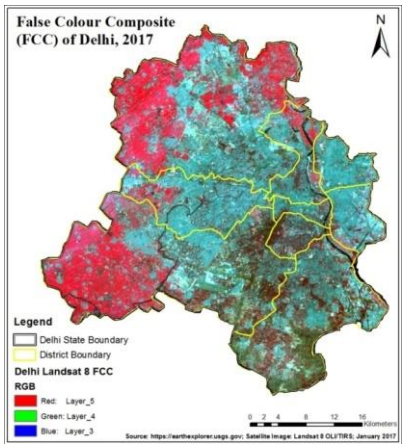

Figure 2: False Color Composite (FCC) of the study area.

Native flora of the ridge includes *Anogeissus pendula, Ziziphus mauritana, Ehretia laevis, and Balanites aegyptiaca* that have been severely invaded by *Prosopis juliflora*. More than 400 bird species have been so far identified in Delhi, including rare ones such as *Pelecanus crispus, Leptoptilos javanicus and Rynchops albicollis* (Urfi, 2003).

2.2. Data Used:

Remotely sensed data in the form of three Landsat 8 OLI/TIRS images (Table 1) was downloaded from USGS website, https://earthexplorer.usgs.gov/. All the satellite images were already georectified. Atmospheric FLAASH correction was applied on all satellite images using ENVI software. After this, the Landsat 8 images were used to carry out land use/land cover classifications and retrieval of biophysical parameters like NDVI, proportion of vegetation, land surface emissivity to estimate the surface temperature.

Table 1: Details of the satellite imagery used in the study.

S. NO.	Satellite	Sensor	Date of Acquisition	Path & Row	Spatial Resolution
1	LANDSAT-8	OLI/TIRS	25-Jun-17	146/40	30 m (100m TIR Band)
2	LANDSAT-8	OLI/TIRS	23-Jan-17	147/40	30 m (100m TIR Band)
3	LANDSAT-8	OLI/TIRS	15-Dec-16	146/40	30 m (100m TIR Band)

2.3. Data Analysis And Processing:

2.3.1. Land Use/Land Cover Data:

The purpose of image classification is to categorize all the pixels in an image into different land cover classes or themes. In this case hybrid technique of image classification was used i.e. the images were first classified using supervised classification technique and then classified output was compared with the respective satellite image and reference data (Toposheets, google earth imagery, etc) was cleaned using recode process in ERDAS IMAGINE software. Accuracy assessment has also been carried out for the LULC thematic maps created.

2.3.2. Data analysis for LST Retrieval:

The algorithm (Figure 4) was employed in ENVI 5.0 and 'Band Math' tool was used for carrying out all the necessary calculations for LST retrieval. The formulas used in this study have been taken from the USGS website (https://landsat.usgs.gov/using-usgs-landsat-8-product) The TIRS band 10 was used in this study for estimation of At-sensor temperature and in further calculations for LST. The metadata of the satellite images used in the algorithm is presented in Figure 3 (only the contants given for Band 10 are used for the calculations).

```
RADIANCE_MULT_BAND_10 = 3.3420E-04
RADIANCE_MULT_BAND_11 = 3.3420E-04
RADIANCE_ADD_BAND_10 = 0.10000
RADIANCE_ADD_BAND_11 = 0.10000
K1_CONSTANT_BAND_10 = 774.8853
K2_CONSTANT_BAND_10 = 1321.0789
K1_CONSTANT_BAND_11 = 480.8883
K2_CONSTANT_BAND_11 = 1201.1442
```

Figure 3: Metadata of Landsat 8 OLI/TIRS satellite images.

2.3.2.1. Top of Atmospheric Spectral Radiance:

OLI and TIRS band data can be converted to TOA spectral radiance using the radiance rescaling factors provided in the metadata file (Figure 3). Landsat 8 Band 10 data is used as input of this calculation. The formula used for conversion of DN numbers to spectral radiance is as follows:

$$L_\lambda = M_L Q_{cal} + A_L \quad \text{... (1)}$$

Where, L_λ represents the TOA spectral radiance, M_L is the Band-specific multiplicative rescaling factor from the metadata (RADIANCE_MULT_BAND_x), A_L is the Band-specific additive rescaling factor from the metadata (RADIANCE_ADD_BAND_x) and Q_{cal} is the atmospherically corrected Band 10 image.

2.3.2.2. Conversion of Radiance to At-Sensor Temperature:

After conversion of DN numbers to Radiance, the spectral radiance is used to calculate the At-sensor temperature/ Brightness Temperature using the thermal constants, i.e., K1 and K2, provided in the metadata file. The following equation has been used to convert Radiance into At-sensor temperature:

$$BT = \frac{K_2}{\ln\left[(K_1/L\lambda) + 1\right]} - 273.15 \quad \text{... (2)}$$

Where, BT is At-satellite brightness temperature, L_λ is TOA spectral radiance, K_1 is Band-specific thermal conversion constant (K1_CONSTANT_BAND_x) and K_2 is Band-specific thermal conversion constant (K2_ CONSTANT_BAND_x). Normally, the resultant brightness temperature comes out in Kelvin, but by subtracting the resultant with 273.15, we are converting the value into Degree Celsius.

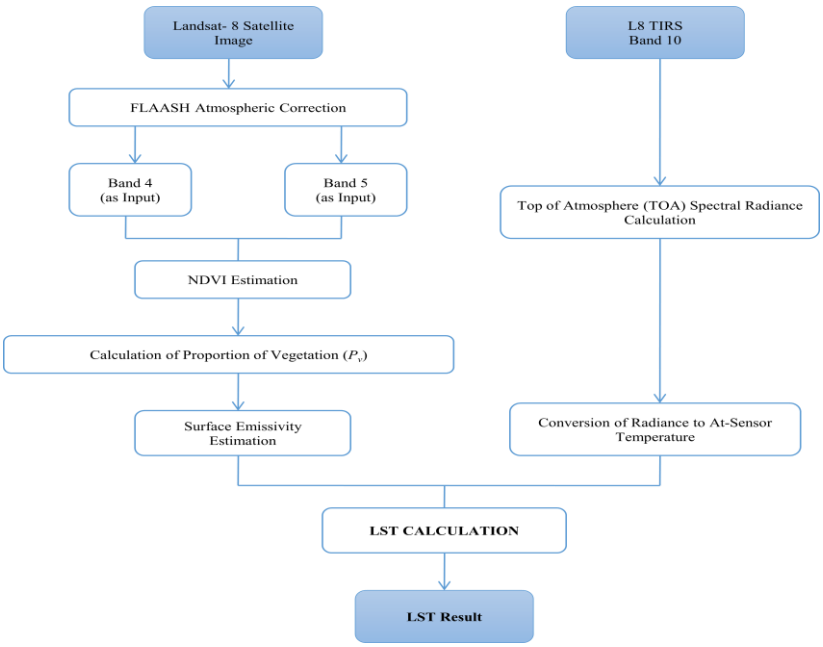

Figure 4: Flowchart showing steps used for LST retrieval.

2.3.2.3. Normalized Difference Vegetation Index (NDVI):

The NDVI is normalization of vegetation difference response. Between Red and Near Infrared region of the EMR. For Landsat 8 images, Band 4 (red) and Band 5 (Near Infrared) are used for estimation of NDVI. For LST retrieval, NDVI calculation is essential as afterwards, proportion of vegetation is calculated from NDVI, which will later be used for Land Surface Emissivity estimation. Since, LST is primarily sensitive to vegetation profile and surface characteristics (emissivity), this step is an essential part of the calculation. The formula used for NDVI calculation is as follows:

$$NDVI = \frac{(NIR - Red)}{(NIR + Red)} \quad \text{... (3)}$$

Where, NIR is the Near Infrared Band of Landsat 8, i.e., Band 5 and Red is band 4 of Landsat 8 data.

2.3.2.4. Calculation of Proportion of Vegetation (*Pv*)

Proportion of vegetation, also known as fractional cover refers to estimating the proportion of an area that is covered by each member of pre-defined set vegetation. NDVI is used in calculation of proportion of vegetation using the formula mentioned below:

$$P_v = (NDVI - NDVI_{min} / NDVI_{max} - NDVI_{min})^2 \quad \text{... (4)}$$

Where, $NDVI_{min}$ is the minimum value of the NDVI range and $NDVI_{max}$ is the maximum value.

2.3.2.5. Calculating Land Surface Emissivity:

Land Surface Emissivity (ε) is a crucial element in LST calculation, since LSE is a proportionality factor that scales blackbody radiance (Plank's Law) to predict emitted radiance, and it is the efficiency of transmitting thermal energy across the surface into the atmosphere (Jiménez-Muñoz et al, 2006). The formula used for emissivity calculation can be described as under:

$$\varepsilon_\lambda = \varepsilon_{v\lambda} P_v + \varepsilon_{s\lambda} (1 - P_v) + C_\lambda \quad \text{... (5)}$$

Where, ε_v and ε_s are the vegetation and soil emissivities, respectively, and C represents the surface roughness taken as a constant value (Avdan & Jovanovska, 2016).

2.3.2.6. Estimation of Land Surface Temperature:

The last step in this process is LST retrieval. Land surface emissivity is one of the key factors of remote sensing retrieving land surface temperature (Li et al, 2015). The following formula has been used for surface temperature estimation:

$$T_S = \frac{BT}{\left[1 + \left(\lambda * \frac{BT}{\rho}\right) * Ln(\epsilon)\right]} \quad \ldots (6)$$

Where, T_s is the LST in degree Celsius, BT is at-sensor brightness temperature, λ is the wavelength of emitted radiance, ρ is the constant = 1.438 x 10^{-2} mK, and ε is the emissivity calculated.

Using these specific sets of equations for LST retrieval, this particular algorithm was applied in ENVI and for further processing of the output ERDAS Imagine and ARCGIS software were used. This algorithm for LST retrieval can only be used to process LANDSAT 8 data, because of the data complexity (Avdan & Jovanovska, 2016). Following the steps of Figure 4, the LST of any Landsat 8 image can be estimated.

3. RESULTS AND DISCUSSION:

For the land use/ land cover classification, the study area was divided in 8 LULC classes (Figure 7). LULC maps were prepared for two time periods viz. January 2017 and June 2017. For January scene, two satellite images were mosaicked and then used for classification. The classification has been carried out based on general/visual understanding of tone and colour of the satellite image, using Google earth imagery and topographical maps of Delhi. According to the LULC map, the built-up area of urban and rural areas of Delhi is about 48.81% of the total geographic area of Delhi. There are seasonal changes in the agricultural activities, for instance, the land is left fallow during the summer months and different crops are grown throughout the year, which is clearly visible in figure 7. Delhi also has a healthy forest and tree cover. According to a study conducted by Sharma (2013), forest and tree cover of Delhi is around 14%. In the current study, scrubland is also added in the LULC class, which is characterised by grass to sparse tree cover. The LULC classes-wise distribution of the area of Delhi along with the graphical representation of the same in January and June 2017 has been given in detail in table 2 and figure 5&6, respectively. Accuracy assessment (Table 3) of the LULC maps has also been carried out via generating random reference points as well as with the help of GCPs collected on ground.

Table 2: Area distribution under Land Use/ Land Cover Classes from classified images of January and June 2017.

S. No.	LULC Class Names	January 2017			June 2017		
		Area (in Hectares)	Area (in km2)	Area (%)	Area (in Hectares)	Area (in km2)	Area (%)
1	Waterbody	1981.8	19.82	1.33	2617.2	26.17	1.76
2	Dense Vegetation	1956.15	19.56	1.31	4615.56	46.16	3.11
3	Open/Sparse Vegetation	2396.97	23.97	1.61	13848.7	138.49	9.33
4	Scrubland	15673.9	156.74	10.53	17796.2	177.96	11.99
5	Agriculture- Cropland	30334.9	303.35	20.39	15956.7	159.57	10.75
6	Agriculture- Fallowland	16066.8	160.67	10.80	28626.4	286.26	19.29
7	Built-up	72619.6	726.20	48.81	63129.1	631.29	42.55
8	Bare Soil	7764.84	77.65	5.22	1787.49	17.87	1.20
	TOTAL	**148794.96**	**1487.95**	**100**	**148377.35**	**1483.7735**	**100**

Figure 5: Area Distribution under different LULC Classes, January 2017

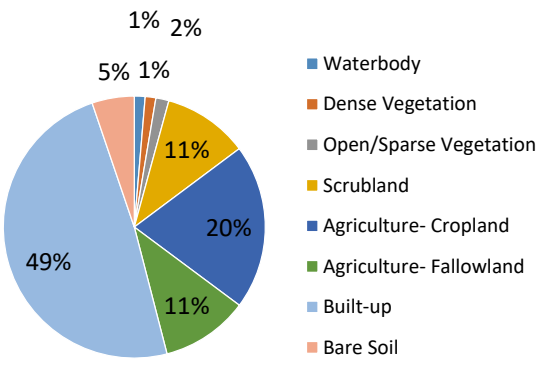

Figure 6: Area Distribution under different LULC Classes, June 2017

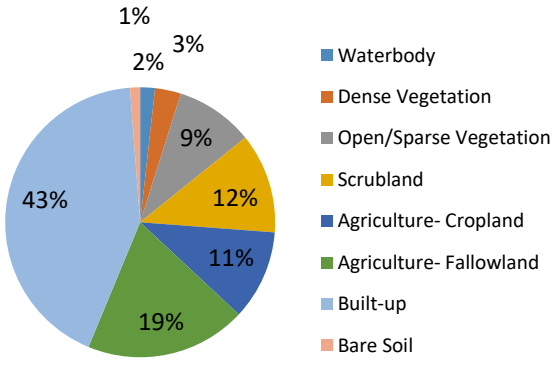

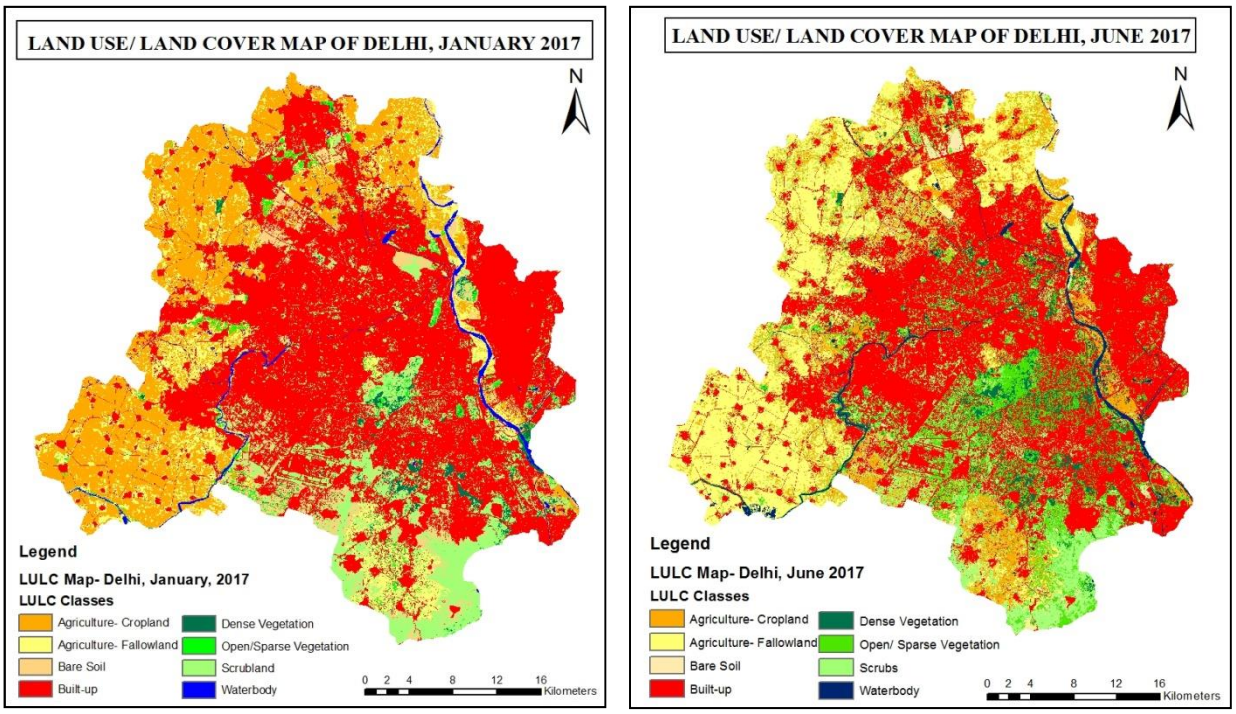

Figure 7: LULC Maps of January 2017 and June 2017.

Table 3: Accuracy Assessment of Supervised Classification.

S. No.	Month/Year	Overall Classification Accuracy	Overall Kappa Statistics
1	January, 2017	83.33%	0.7688
2	June, 2017	85%	0.7877

The study results of LST show that the surface temperature varies on the basis of existing land use/ Cover and Vegetation cover. In this study, season-wise changes of surface temperature patterns w.r.t. the general LULC patterns through the surface temperature maps are explored (Figure 8).

The mean LST value for Delhi in January and June 2017 was estimated to be 20.68 ˚C and 29.64 ˚C, respectively. The statistics of the LST and NDVI generated is given in table 4. In summer, LST ranged from 24.31˚C to 35.32˚C and in winter from 18.31˚C to 23.97˚C, which is much influenced by the existing Land Use/Covers. During summer, the lowest temperature was recorded from surface waterbodies, and the highest temperature was recorded from barren agricultural land and dense urban areas.

Table 4: Mean, Min and Max LST and NDVI over Delhi.

Statistics	January LST	January NDVI	June LST	June NDVI
Mean	20.68	0.2777	29.64	0.2171
Min	18.31	-0.4144	24.31	-0.1738
Max	23.97	0.8078	35.32	0.7671

However, an ideal UHI pattern was observed during winter. During winter, the high surface temperature areas are observed mostly in the central and southern part of Delhi and as per the lulc maps created, most of the built-up area is concentrated in Central, Southern and South-eastern part of Delhi. Though, the UHI Intensity during winters is comparatively less, i.e., 2.9˚C, which is comparatively less than that of summer 2017, i.e., 3.6˚C, there is an ideal UHI pattern observed during this time (Figure 7). Even so, the Central Delhi Region and the commercial/industrial areas displayed heat island conditions in summer and winter seasons, with a mean temperature difference of 3.6˚C and 2.9˚C, respectively, compared to the suburbs.

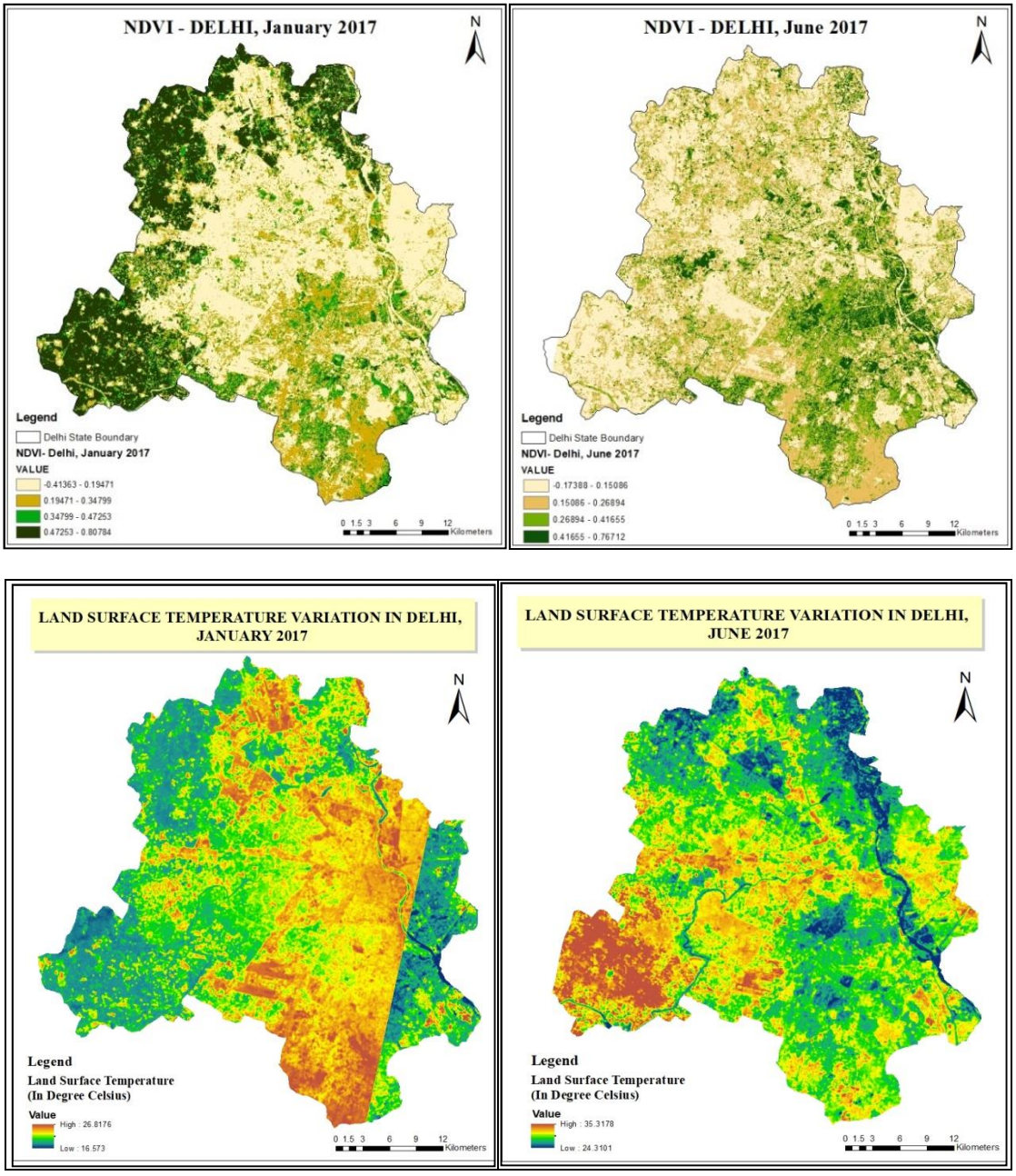

Figure 8: NDVI and LST distribution over Delhi in January and June 2017.

The lowest temperature in winter, i.e. 18.31˚C is shown in the south-western parts of Delhi, which is mostly agricultural land, whereas the lowest temperature during summer, i.e., 24.31˚C is shown in mostly parts of Yamuna and in certain 'Cool Islands' observed in the urban areas of Delhi. Mostly, these cool islands observed during summer in urban areas area either surrounded by good vegetation or have comparatively less concretized surfaces. Some of these cool islands include the Central Ridge area (26.3˚C), India Gate premises (27.4˚C), Deer Park- Hauz Khas (26.2˚C), Nehru Memorial Museum and Library (27.2˚C), etc. Other than this, it is clear in figure 6 that there is an apparent correlation between LST and NDVI from the visual interpretation of LST and NDVI contrasts. Mean LST and NDVI values associated with different land-use types are always significantly different (Yeu et al, 2007).

Table 5: LST range (in Degree Celsius) over Delhi in January and June 2017.

S. No.	LST Level	LST range- January	LST range- June
1	Low	18.31 - 20.20	24.31 - 26.47
2	Medium	20.20 - 22.08	26.47 - 29.66
3	High	22.08 - 23.97	29.66 - 35.32

Table 6: Table showing range of LST in the built-up area of Delhi.

S. No.	Month/Year	LULC Type	Area (in square km)	LST range (in Degree Celsius)	LST Level
1	January, 2017	Built-up	726.196	19.2 - 23.52	Medium- High
2	June, 2017	Built-up	631.29	28.4 - 34.2	~ High

In table 5, LST has been categorized into three categories just to compare the LST range difference in both the seasons. Also, the lulc map created was used for extraction of LST over the built-up area in Delhi, which is mentioned in table 6. There is also a difference in built-up area between the two months, which can be accounted to the difference in extent of the tiles downloaded from the USGS website (path and row difference). In the table 6, it is clear that built-up is among the hottest surface types in both summer and winter seasons, which clearly demonstrates the presence of UHI phenomenon over Delhi.

4. CONCLUSION:

This study demonstrated the development of Urban Heat Island phenomenon and its seasonal variations over Delhi metropolitan area. Though, landsat-based estimations of impervious surface are always subject to seasonal and phonological variations, the results of the study suggest that in the urban area of Delhi, the surface temperature observed is comparatively higher than the surface temperature of rural area. Furthermore, the surface temperature increment at the city level is mainly due to the joint effect of anthropogenic activities, changes in LULC patterns and vegetation.

5. REFERENCES:

1. Avdan, U., & Jovanovska, G. (2016). Algorithm for Automated Mapping of Land Surface Temperature Using LANDSAT 8 Satellite Data. *Journal of Sensors*, *2016*, 1-8.
2. Bhati, S., & Mohan, M. (2015). WRF model evaluation for the urban heat island assessment under varying land use/land cover and reference site conditions. *Theoretical and Applied Climatology*, 1-16.
3. Delhi Population. (2017). *Worldpopulationreview.com*. Retrieved 21 September 2017, from http://world populationreview.com/world-cities/Delhi-population/
4. Dhorde, A., Dhorde, A., & Gadgil, A. S. (2009). Long-term temperature trends at four largest cities of India during the twentieth century. *J. Indian Geophys. Union*, *13*(2), 85-97.
5. *How are the Thermal Infrared Sensor (TIRS) thermal bands aboard Landsat 8 used? | Landsat Missions*. (2017). *Landsat.usgs.gov*. Retrieved 22 August 2017, from https://landsat.usgs.gov/how-are-thermal-infrared-sensor-tirs-thermal-bands-aboard-landsat-8-used
6. India State of Forest Report. (2013). Forest Survey of India, Ministry of Forests and Environment, Govt. of India.
7. India State of Forest Report. (2015). Forest Survey of India, Ministry of Environment, Forests and Climate Change, Govt. of India.
8. Jiménez-Muñoz, J. C., Sobrino, J. A., Gillespie, A., Sabol, D., & Gustafson, W. T. (2006). Improved land surface emissivities over agricultural areas using ASTER NDVI. *Remote Sensing of Environment*, *103*(4), 474-487.
9. Kikon, N., Singh, P., Singh, S. K., & Vyas, A. (2016). Assessment of urban heat islands (UHI) of Noida City, India using multi-temporal satellite data.*Sustainable Cities and Society*, *22*, 19-28.
10. Li, Y., Yang, K. and Yang, R. (2015). "Land surface temperature estimation from remote sensing data - a case study in Kun Ming city," *2015 23rd International Conference on Geoinformatics*, Wuhan, 2015, pp. 1-6.
11. Lo, C. P., & Quattrochi, D. A. (2003). Land-Use and land-cover change, urban heat island phenomenon, and health implications. *Photogrammetric Engineering & Remote Sensing*, 69(9), 1053-1063.
12. Mallick, J. (2014). Land characterization analysis of surface temperature of semi-arid mountainous city Abha, Saudi Arabia using remote sensing and GIS. *Journal of Geographic Information System*, *6*(6), 664.
13. Mallick, J., & Rahman, A. (2012). Impact of population density on the surface temperature and micro-climate of Delhi. *CurrSci*, *102*, 12.
14. McDonnell, M. J., Pickett, S. T., Groffman, P., Bohlen, P., Pouyat, R. V., Zipperer, W. C., Parmelee R.W., Carreiro M.M. & Medley, K. (1997). Ecosystem processes along an urban-to-rural gradient. *Urban Ecosystems*, *1*(1), 21-36.
15. Montanaro, M., Gerace, A., Lunsford, A., & Reuter, D. (2014). Stray light artifacts in imagery from the Landsat 8 Thermal Infrared Sensor. *Remote Sensing*, *6*(11), 10435-10456.
16. Oke, T. R. (1982). The energetic basis of the urban heat island. *Quarterly Journal of the Royal Meteorological Society*, *108*(455), 1-24.

17. Roy, S. S., & Singh, R. B. (2015). Role of local level relative humidity on the development of urban heat island across the Delhi Metropolitan Region. In *Urban Development Challenges, Risks and Resilience in Asian Mega Cities* (pp. 99-118). Springer Japan.
18. Sharma, R. (2013). Development and Behaviour of Surface Urban Heat Island (SUHI) in semi-arid conditions of Delhi. PhD Thesis, Teri University, New Delhi, India, December 2013.
19. Sharma, R., & Joshi, P. K. (2015). The Changing Urban Landscape and Its Impact on Local Environment in an Indian Megacity: The Case of Delhi. In *Urban Development Challenges, Risks and Resilience in Asian Mega Cities* (pp. 61-81). Springer Japan.
20. Singh, R. B. (Ed.). (2015). *Urban development challenges, risks and resilience in Asian Mega Cities*. Springer.
21. Singh, R. B., & Grover, A. (2015). Spatial correlations of changing land use, surface temperature (UHI) and NDVI in Delhi using Landsat satellite images. In *Urban Development Challenges, Risks and Resilience in Asian Mega Cities* (pp. 83-97). Springer Japan.
22. Singh, R. B., Grover, A., & Zhan, J. (2014). Inter-seasonal variations of surface temperature in the urbanized environment of Delhi using Landsat thermal data. *Energies*, *7*(3), 1811-1828.
23. Sinha, G.N. (Ed.) (2014). *An Introduction to the Delhi Ridge*. Department of Forests & Wildlife, Govt. of NCT of Delhi, New Delhi. xxiv+154 pp.
24. Statistical abstract of Delhi. (2014). Directorate of Economics & Statistics, Govt. of NCT of Delhi.
25. Urfi, A. J. (2003) The birds of Okhla Barrage Bird Sanctuary, Delhi, India. *Forktail*19: 39-50.
26. *Using the USGS Landsat 8 Product | Landsat Missions*. (2017). *Landsat.usgs.gov*. Retrieved 23-08-20172017, from https://landsat.usgs.gov/using-usgs-landsat-8-product
27. Yu, X., Guo, X., & Wu, Z. (2014). Land surface temperature retrieval from Landsat 8 TIRS—Comparison between radiative transfer equation-based method, split window algorithm and single channel method. *Remote Sensing*, *6*(10), 9829-9852.
28. Yue, W., Xu, J., Tan, W., & Xu, L. (2007). The relationship between land surface temperature and NDVI with remote sensing: application to Shanghai Landsat 7 ETM+ data. *International Journal of Remote Sensing*, *28*(15), 3205-3226.